International Journal of Solids and Structures 46 (2009) 1648–1658

Contents lists available at ScienceDirect

International Journal of Solids and Structures

journal homepage: www.elsevier.com/locate/ijsolstr

Edge-cracked bimaterial systems under thermal heating

Abd El-Fattah A. Rizk [a], Meftah Hrairi [b,*]

[a] Department of Science in Engineering, International Islamic University Malaysia, P.O. Box 10, 50728 Kuala Lumpur, Malaysia
[b] Department of Mechanical Engineering, International Islamic University Malaysia, P.O. Box 10, 50728 Kuala Lumpur, Malaysia

ARTICLE INFO

Article history:
Received 26 August 2008
Received in revised form 28 November 2008
Available online 24 December 2008

Keywords:
Thermoelasticity
Bimaterial systems
Edge crack
Stress intensity factor

ABSTRACT

The problem of thermoelastic edge-cracking in two-layered bimaterial systems subjected to convective heating is considered. The medium is assumed to be insulated on one surface and exposed to sudden convective heating on another surface containing the edge crack. It is known that, when a bimaterial system's surface is heated, compressive stresses arise near the heating surface, forcing the crack surfaces together over a certain cusp-shaped contact length. It is also known that, for a cooled bimaterial systems surface, tensile stresses take place close to the cooling surface and tend to open the crack. So, the edge cracked heating surface problem is treated as an embedded crack with a smooth closure condition of the crack surfaces, with the crack contact length being an additional unknown variable. Superposition and uncoupled quasi-static thermoelasticity principles are adopted to formulate the problem. By using a Fourier integral transform technique, the mixed boundary value problem is reduced to a Cauchy type singular integral equation with an unknown function as the derivative of the crack surface displacement. The numerical results of the stress intensity factors for an edge crack and a crack terminating at the interface, are calculated and presented as a function of time, crack length, heat transfer coefficient, and thickness ratio for two different bimaterial systems, namely a stainless steel layer welded on ferritic steel and a ceramic layer coating on ferritic steel.

1. Introduction

The study of thermoelastic crack problems in multi-layered components has been undertaken by a number of researchers since it is pertinent to many engineering applications. For example, ceramic thermal barrier coating is used in jet engines, stainless steel cladding is used in pressure vessels and pipes, and a variety of bonded materials are used in microelectronic devices. The study of a cracked elastic plate subjected to thermal stresses due to surface cooling and heating have been considered (Nied, 1983, 1987; Lam et al., 1992; Fan and Yu, 1992; Rizk, 1993; Rizk and Radwan, 1993; Rizk, 2004, 2005). Crack problems in multi-layered materials under thermal loading have also been investigated by many researchers (Rizk and Erdogan, 1989; Erdogan and Rizk, 1992; Itou and Rengen, 1993; Choi et al., 1995, 1998; Ikeda and Sun, 2001; Choi, 2003; Itou, 2004; Rizk, 2008).

Thermal stresses may be generated by sudden cooling or heating of the surface of bimaterial systems. Most often, the mechanical and thermal properties within the bimaterial systems are different; resulting in very high thermal stresses and leading to severe damage, especially in the presence of preexisting cracks. The most important mode of mechanical failure is subcritical crack propagation. This requires the determination of the stress intensity factor as a function of time and crack length as well as the material combination properties of the bimaterial systems. It is important to note that the analysis of the problem under surface cooling is different than the analysis under surface heating. The thermal shock of the bimaterial systems subjected to surface cooling was considered in Rizk (2008) in which very high tensile stresses take place close to the cooled surface, which tend to open the crack surfaces. In the case of surface heating, compressive stresses are generated near the heated surface, forcing the crack surfaces to come into contact along a certain contact length. By taking the crack contact length into consideration, the crack will be cusp-shaped and a smooth closure condition of the crack surfaces can be applied in the analysis (Bakioglu et al., 1976). So, the problem is considered to be an embedded crack problem with smooth closure conditions at the crack surfaces. The crack contact length is an additional unknown parameter that will be determined iteratively. This is known as a non-linear crack contact problem.

In this work, the analysis of two-layered bimaterial systems shown in Fig. 1, containing an edge crack ($b < h_1$) and crack terminating at the interface ($b = h_1$) normal to the interface, and that is subjected to convective heating on the surface containing the crack ($x = 0$) is investigated. It is assumed that the bimaterial systems consist of two dissimilar linear isotropic homogeneous materials bonded along an ideal plane interface. Also, the problem is treated as an uncoupled quasi-static isothermal problem, i.e. the inertia effects are negligible and the thermoelastic coupling effects and

* Corresponding author. Tel.: +603 6196 4581; fax: +603 6196 4455.
E-mail address: meftah@iiu.edu.my (M. Hrairi).

0020-7683/$ - see front matter © 2008 Elsevier Ltd. All rights reserved.
doi:10.1016/j.ijsolstr.2008.12.003

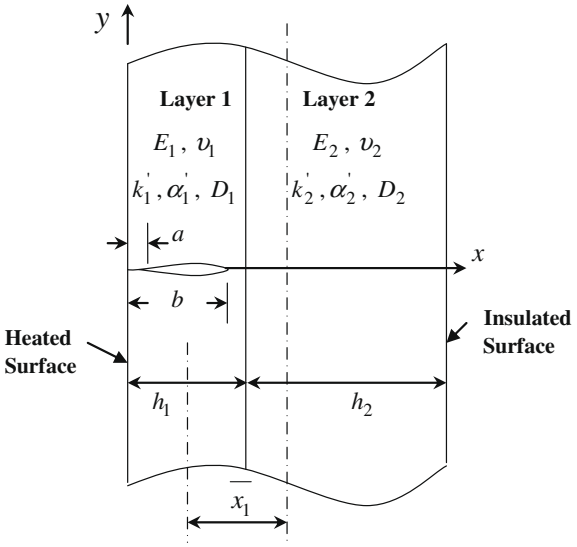

Fig. 1. Crack geometry in the bimaterial systems under surface heating.

possible dependence of the thermoelastic coefficients on the temperature are also negligible. Since the problem is linear, the superposition technique can be applied since the stress state of the final solution is considered to be the sum of two solutions. The first solution component consists of the transient thermal stresses for the bimaterial plate in the absence of a crack. The second solution component is obtained by considering the solution of the isothermal cracked problem (mixed boundary value problem) using the thermal stresses obtained from the first component solution with equal and opposite sign applied on the crack surfaces as the only external loads. Since our interest is to determine the stress intensity factors, it is sufficient to consider the stresses obtained only from the cracked problem (perturbation problem). The Fourier integral transform is used to formulate the cracked problem. By expressing the displacement components in terms of a Fourier integral transform, the problem will be reduced to a singular integral equation of the Cauchy type with an unknown function that is defined as the derivative of the crack surface displacement. The resulting singular integral equation is solved numerically using the expansion method developed in Kaya and Erdogan (1987a,b). The numerical results of the stress intensity factors are calculated for both an edge crack and a crack terminating at the interface as a function of normalized time, normalized crack length, normalized coefficient of heat transfer, and the thickness ratio for two different bimaterial systems combinations – called system A and system B. System A represents a stainless steel layer (layer 1) welded on ferritic steel (layer 2) with similar mechanical properties but different thermal properties while system B corresponds to a ceramic coating layer (layer 1) bonded to ferritic steel (layer 2) in which the mechanical and the thermal properties of the materials are different.

2. Mathematical formulation

Fig. 1 illustrates the thermoelastic bimaterial systems for a mathematical formulation. It is composed of two layers of dissimilar materials with different thermoelastic properties. Layer 1, of thickness h_1, containing a crack of length $l = (b - a)$ normal to the interface, is bonded to layer 2, of thickness h_2. The medium is initially assumed at homogenous temperature T_o. At $t \geqslant 0$, the plane $x = 0$ is subjected to sudden convective heating with ambient temperature T_a while the other boundary $x = h_1 + h_2$ is assumed to be insulated. The superposition technique is used to formulate the problem where the total stress state is the sum of the two solutions. First, the transient thermal stress solution is obtained for the thermal uncracked medium. Second, the solution of the isothermal cracked medium (mixed boundary value problem) is obtained using the equal and opposite sign of the thermal stresses obtained from the uncracked medium as the crack surface tractions. Since the temperature distribution and the transient thermal stresses of the uncracked medium are independent of whether the medium is heated or cooled, the transient temperature and the transient thermal stresses for the uncracked medium can be obtained from Rizk (2008). So, the temperature distribution may be written as

$$\frac{\theta_1(x^*,\tau)}{\theta_o} = 1 - 2\sum_{n=1}^{\infty}\frac{1}{\lambda_n}\frac{e^{-\tau\lambda_n^2}[\cos\lambda_n(x^*-1)\cos(\delta R\lambda_n)+\eta\sin\lambda_n(x^*-1)\sin(\delta R\lambda_n)]}{[(\lambda_n/Bi)(1+\eta\delta R)\cos\lambda_n\cos(\delta R\lambda_n)-(\lambda_n/Bi)(\eta+\delta R)\sin\lambda_n\sin(\delta R\lambda_n)}$$
$$\frac{1}{+((1/Bi)+1+\eta\delta R)\sin\lambda_n\cos(\delta R\lambda_n)+((\eta/Bi)+\delta R+\eta)\cos\lambda_n\sin(\delta R\lambda_n)]}, \quad 0\leqslant x^*\leqslant 1 \tag{1}$$

$$\frac{\theta_2(x^*,\tau)}{\theta_o} = 1 - 2\sum_{n=1}^{\infty}\frac{1}{\lambda_n}\frac{e^{-\tau\lambda_n^2}[\cos\delta\lambda_n(x^*-1)\cos(\delta R\lambda_n)+\sin\delta\lambda_n(x^*-1)\sin(\delta R\lambda_n)]}{[(\lambda_n/Bi)(1+\eta\delta R)\cos\lambda_n\cos(\delta R\lambda_n)-(\lambda_n/Bi)(\eta+\delta R)\sin\lambda_n\sin(\delta R\lambda_n)}$$
$$\frac{1}{+((1/Bi)+1+\eta\delta R)\sin\lambda_n\cos(\delta R\lambda_n)+((\eta/Bi)+\delta R+\eta)\cos\lambda_n\sin(\delta R\lambda_n)]}, \quad 1\leqslant x^*\leqslant 1+R \tag{2}$$

where $\theta_i(x,t) = T_i(x,t) - T_o$, $(i = 1,2)$, $\theta_o = T_a - T_o$, $x^* = x/h_1$, $\tau = tD_1/h_1^2$ is called the Fourier number (Pecht, 1991; Zudin, 2007), $\eta = (k_2'/k_1')\sqrt{D_1/D_2}$, $R = h_2/h_1$ (thickness ratio), $\delta = \sqrt{D_1/D_2}$, $Bi = hh_1/k_1'$ is the Biot number (Pecht, 1991; Zudin, 2007), h is the coefficient of heat transfer, and k_i', D_i $(i = 1,2)$ are the coefficients of thermal conductivity and the thermal diffusivity, respectively, and λ_n are the roots of the transcendental equation

$$Bi[\cos\lambda_n\cos(\delta R\lambda_n) - \eta\sin\lambda_n\sin(\delta R\lambda_n)] = \lambda_n[\sin\lambda_n\cos(\delta R\lambda_n) + \eta\cos\lambda_n\sin(\delta R\lambda_n)] \tag{3}$$

and the transient thermal stresses may be given by

$$\sigma_{iyy}^T(x,t) = \sigma_{izz}^T(x,t) = \frac{E_i}{1-\upsilon_i}\left[\varepsilon_o(t) + \frac{x}{\rho(t)} - \alpha_i'\theta_i(x,t)\right] \quad (i = 1,2), \tag{4}$$

where E_i, υ_i, α_i', $(i = 1,2)$, are the Young modulus, the Poisson ratio, and the coefficient of linear thermal expansion, respectively, $\varepsilon_o(t)$ is the uniform strain that is given by

$$\varepsilon_o = \frac{\left(\frac{E_1}{1-\upsilon_1}\right)\alpha_1' h_1\overline{\theta}_1 + \left(\frac{E_2}{1-\upsilon_2}\right)\alpha_2' h_2\overline{\theta}_2}{\left(\frac{E_1}{1-\upsilon_1}\right)h_1 + \left(\frac{E_2}{1-\upsilon_2}\right)h_2}, \tag{5}$$

where

$$\overline{\theta}_1 = \frac{1}{h_1}\int_0^{h_1}\theta_1(x,t)dx, \quad \overline{\theta}_2 = \frac{1}{h_2}\int_{h_1}^{h_1+h_2}\theta_2(x,t)dx \tag{6}$$

and the curvature $1/\rho$ is given by

$$\frac{1}{\rho} = \frac{-(\overline{x}_1 + \frac{h_1}{2})\left[\left(\frac{E_1}{1-\upsilon_1}\right)\alpha_1' h_1\overline{\theta}_1 + \left(\frac{E_2}{1-\upsilon_2}\right)\alpha_2' h_2\overline{\theta}_2\right] + \left(\frac{E_1}{1-\upsilon_1}\right)\alpha_1' M_{t1} + \left(\frac{E_2}{1-\upsilon_2}\right)\alpha_2' M_{t2}}{\left(\frac{E_1}{1-\upsilon_1}\right)I_1 + \left(\frac{E_2}{1-\upsilon_2}\right)I_2 + \left(\frac{E_1}{1-\upsilon_1}\right)\frac{(h_1+h_2)}{2}h_1\overline{x}_1}, \tag{7}$$

where $I_1 = h_1^3/12$, $I_2 = h_2^3/12$ are the moment of inertia about the centroidal axes of layer 1 and layer 2, respectively, and

$$M_{t1} = \int_0^{h_1}\theta_1(x,t)x\,dx, \quad M_{t2} = \int_{h_1}^{h_1+h_2}\theta_2(x,t)x\,dx,$$
$$\overline{x}_1 = \frac{(h_1+h_2)}{2}\frac{\left(\frac{E_2}{1-\upsilon_2}\right)h_2}{\left(\frac{E_1}{1-\upsilon_1}\right)h_1 + \left(\frac{E_2}{1-\upsilon_2}\right)h_2}, \tag{8}$$

where $\bar{x}_1$ is the distance between the centroidal axis of layer 1 and the bending axis (isothermal plane, $\theta_1 = \theta_2$, Burgreen, 1971). Referring to Fig. 1, the solution of the plane elasticity problem is required to solve the following governing differential equations for the displacements:

$$(\kappa_i - 1)\nabla^2 u_i + 2\left(\frac{\partial^2 u_i}{\partial x^2} + \frac{\partial^2 v_i}{\partial x \partial y}\right) = 0 \quad (i = 1, 2), \tag{9}$$

$$(\kappa_i - 1)\nabla^2 v_i + 2\left(\frac{\partial^2 u_i}{\partial x \partial y} + \frac{\partial^2 v_i}{\partial y^2}\right) = 0 \quad (i = 1, 2), \tag{10}$$

where $\kappa_i = (3 - 4\upsilon_i)$, $(i = 1, 2)$, for plane strain, and u_i, v_i, $(i = 1, 2)$, are the x and y components of the displacement vectors, respectively. Since $y = 0$ is a plane of symmetry, then the problem will be considered for $0 < y < \infty$ which is subjected to the following conditions:

Table 1
Thermoelastic properties of the bimaterial systems used in the numerical results.

Bimaterial systems	k_2'/k_1'	D_2/D_1	α_2'/α_1'	E_2/E_1	υ_2/υ_1
A	3	3	0.75	1	1
B	3.385	4.07	2.2939	0.6111	1

$$\sigma_{1xx}(0, y) = 0, \quad \sigma_{1xy}(0, y) = 0, \tag{11}$$

$$\sigma_{1xx}(h_1, y) = \sigma_{2xx}(h_1, y), \quad \sigma_{1xy}(h_1, y) = \sigma_{2xy}(h_1, y), \tag{12}$$

$$u_1(h_1, y) = u_2(h_1, y), \quad v_1(h_1, y) = v_2(h_1, y), \tag{13}$$

$$\sigma_{2xx}(h_1 + h_2, y) = 0, \quad \sigma_{2xy}(h_1 + h_2, y) = 0, \tag{14}$$

$$\sigma_{1xy}(x, 0) = 0, \ 0 < x < h_1 \quad \text{and} \quad \sigma_{2xy}(x, 0) = 0,$$

$$v_2(x, 0) = 0, \ h_1 < x < h_1 + h_2, \tag{15}$$

$$u_i(x, y) \to 0, \ v_i(x, y) \to 0, \quad (i = 1, 2) \text{ as } y \to \infty, \tag{16}$$

$$v_1(x, 0) = 0, \ 0 < x < a, \ b < x < h_1,$$

$$\sigma_{1yy}(x, 0) = -\sigma_{1yy}^T(x, t), \ a < x < b, \tag{17}$$

where $\sigma_{1ij}(x, y)$, $\sigma_{2ij}(x, y)$, $(i, j = x, y)$, are the stresses in layer 1 and layer 2, respectively, and $\sigma_{1yy}^T(x, t)$ is the thermal stress obtained from the uncracked problem. Differential equations (9) and (10) can be solved by expressing the displacement components u_i, v_i $(i = 1, 2)$ in terms of the Fourier integral transform, i.e.

$$u_i(x, y) = \frac{2}{\pi}\int_0^\infty A_i(x, \alpha)\cos \alpha y \, d\alpha + \frac{1}{2\pi}\int_{-\infty}^{\infty} B_i(y, \beta) e^{ix\beta} \, d\beta \quad (i = 1, 2), \tag{18}$$

$$v_i(x, y) = \frac{2}{\pi}\int_0^\infty F_i(x, \alpha)\sin \alpha y d\alpha + \frac{1}{2\pi}\int_{-\infty}^{\infty} G_i(y, \beta) e^{ix\beta} \, d\beta \quad (i = 1, 2), \tag{19}$$

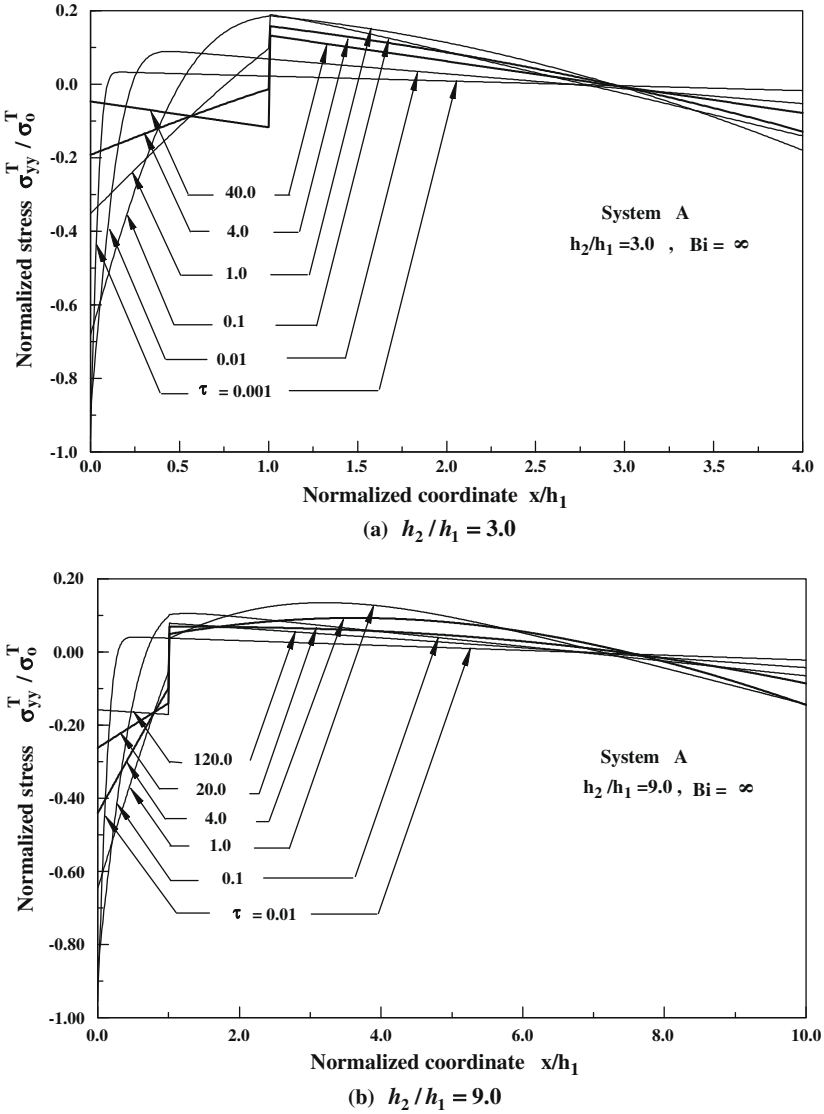

Fig. 2. Normalized thermal stresses for bimaterial system A at different Fourier number for Biot number $Bi = \infty$.

where A_i, B_i, F_i, G_i $(i = 1, 2)$ are the unknown functions to be determined. Substituting Eqs. (18) and (19) into Eqs. (9) and (10), and solving the resulting ordinary differential equations and using the stress–displacement relations with the conditions specified by Eqs. (11)–(17) and defining a new unknown function $\varphi(x) = \partial v_1(x,0)/\partial x$, the problem will be reduced to, after lengthy but straightforward manipulations, the following singular integral equation of the unknown function $\varphi(x)$:

$$\int_a^b \frac{\varphi(s)}{(s-x)}ds + \int_a^b k_1(x,s)\varphi(s)ds = -\frac{\pi(\kappa_1+1)}{4\mu_1}\sigma^T_{1yy}(x,t), \quad a < x < b, \tag{20}$$

where the kernel $k_1(x,s)$ can be found in Rizk (2008). It can be seen that as long as the crack is away from the free surface $(a > 0)$ and the interface $(b < h_1)$, the kernel $k_1(x,s)$ is bounded and the singular integral equation (20) has only a Cauchy singularity. In the limiting cases for an edge crack $(a = 0)$ and crack terminating at the interface $(b = h_1)$, some terms in the kernel $k_1(x,s)$ become unbounded and would contribute to the singular behavior of the solution. So, the kernel $k_1(x,s)$ may be written in the form (Rizk, 2008)

$$k_1(x,s) = k_1^b(x,s) + k_{1a}^s(x,s) + k_{1b}^s(x,s), \tag{21}$$

where $k_1^b(x,s)$ is bounded in the interval $[a,b]$ including $a = 0$ and $b = h_1$, and $k_{1a}^s(x,s)$ and $k_{1b}^s(x,s)$ are the singular terms as $a = 0$ and $b = h_1$, respectively, and they are found to be

$$k_{1a}^s(x,s) = -\frac{1}{s+x} + \frac{6x}{(s+x)^2} - \frac{4x^2}{(s+x)^3}, \tag{22}$$

$$k_{1b}^s(x,s) = \frac{c_{11}}{2h_1 - x - s} + \frac{c_{12}(h_1 - x)}{(2h_1 - x - s)^2} + \frac{c_{13}(h_1 - x)^2}{(2h_1 - x - s)^3}, \tag{23}$$

where

$$c_{11} = \frac{3(m-1)}{2(m+\kappa_1)} - \frac{(m\kappa_2 - \kappa_1)}{2(m\kappa_2 + 1)}, \quad c_{12} = -6\frac{m-1}{m+\kappa_1}, \quad c_{13} = 4\frac{m-1}{m+\kappa_1}, \quad m = \frac{\mu_1}{\mu_2}. \tag{24}$$

Such kernels are called generalized Cauchy kernels.

The singular behavior of the solution of the singular integral equation (20) at the irregular points a and b can be examined by following the Muskhelishvili technique (1953) using the function theoretic method. Let the unknown function $\varphi(s)$ be expressed as

$$\varphi(s) = \frac{g(s)}{(s-a)^{\gamma_1}(b-s)^{\gamma_2}}, \tag{25}$$

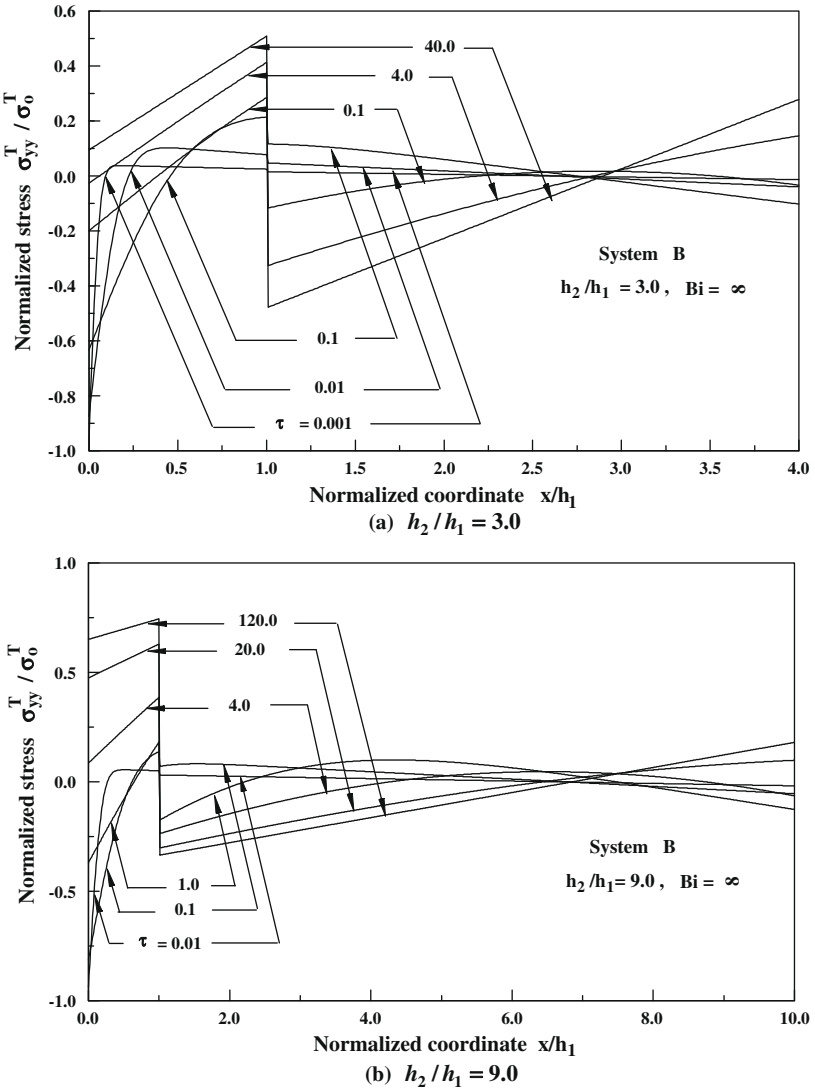

Fig. 3. Normalized thermal stresses for bimaterial system B, at different Fourier number for Biot number $Bi = \infty$.

where $g(s)$ is a bounded function in the closed interval $[a,b]$ and nonzero at the end points a and b, and γ_1, γ_2 are the strength of the singularity at the end points which should satisfy $0 < Re(\gamma_1,\gamma_2) < 1$. Following Muskhelishvili (1953), as long as we have an embedded crack in layer 1 ($a > 0,\ b < h_1$), the singularities at the crack tips a and b are found to be $\gamma_1 = 1/2$ and $\gamma_2 = 1/2$. While in the case of an edge crack ($a = 0,\ b < h_1$), the singularity at the crack tip b is $\gamma_2 = 1/2$ and the singularity at the crack tip $a = 0$ would satisfy the following characteristic equation:

$$\cos\pi\gamma_1 - 2(\gamma_1 - 1)^2 + 1 = 0, \tag{26}$$

which has only one acceptable root given by $\gamma_1 = 0$. For the case of crack terminating at the interface ($b = h_1$), the singularity γ_2 at the tip $b = h_1$ would depend on the material properties and its characteristic equation will be given by Rizk and Erdogan (1989)

$$\cos\pi\gamma_2 - \frac{1}{2}c_{13}\gamma_2(\gamma_2+1) - c_{12}\gamma_2 - c_{11} = 0, \tag{27}$$

where c_{11}, c_{12}, c_{13} are given by Eq. (24).

Our interest is to calculate the stress intensity factors for Mode I which are defined at the crack tips a and b as

$$K(a) = \lim_{x\to a^-}\sqrt{2(a-x)}\sigma_{1yy}(x,0), \tag{28}$$

$$K(b) = \lim_{x\to b^+}\sqrt{2(x-b)}\sigma_{1yy}(x,0), \tag{29}$$

in which $\sigma_{1yy}(x,0)$ is the stress outside the crack in layer 1. Note that Eq. (20) gives the stresses inside and outside the crack. Following Muskhelishvili (1953) and using Eqs. (20) and (25), the stress intensity factors for an embedded crack at a and b are given by

$$K(a) = \frac{4\mu_1}{\kappa_1+1}\left(\frac{2}{b-a}\right)^{1/2} g(a), \tag{30}$$

$$K(b) = -\frac{4\mu_1}{\kappa_1+1}\left(\frac{2}{b-a}\right)^{1/2} g(b), \tag{31}$$

and for an edge crack ($a = 0,\ b < h_1$), the stress intensity factor at the crack tip b is given by

$$K(b) = -\frac{4\mu_1}{\kappa_1+1}\sqrt{2}g(b). \tag{32}$$

For the crack terminating at the interface ($b = h_1$), the stress intensity factor at b is defined by

$$K(b=h_1) = \lim_{x\to h_1^+}\sqrt{2}(x-h_1)^{\gamma_2}\sigma_{2yy}(x,0), \tag{33}$$

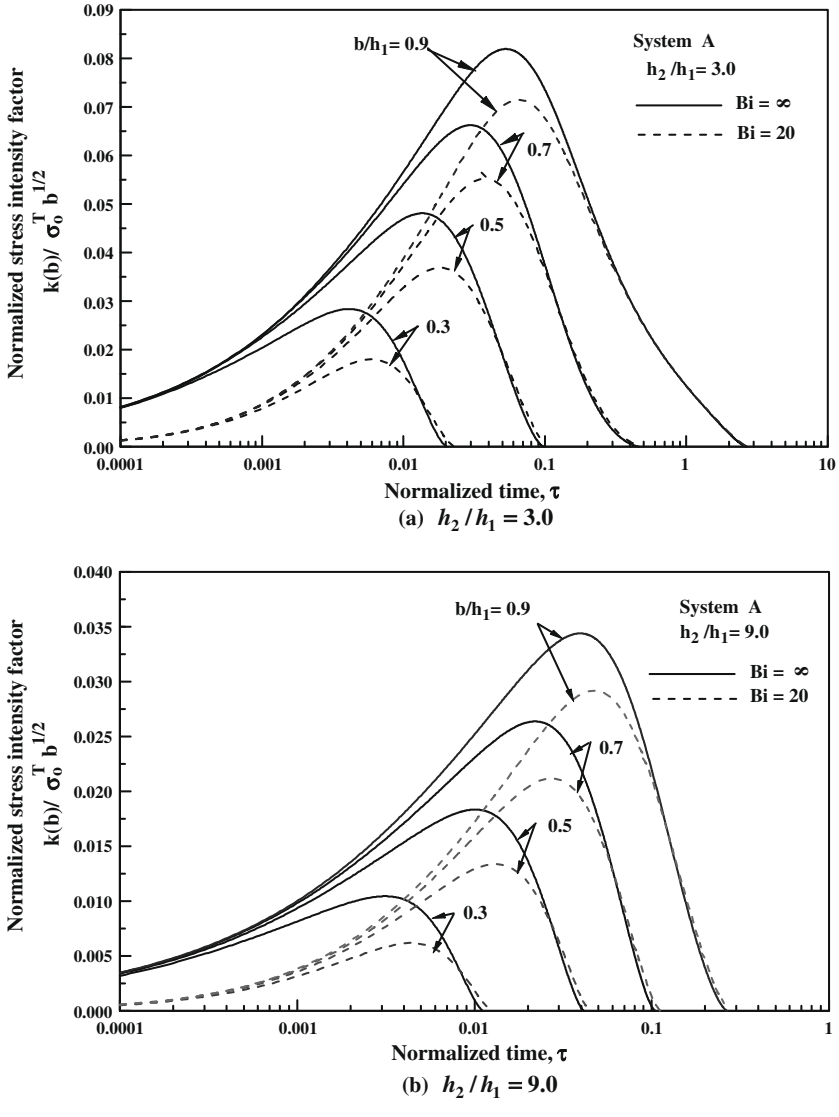

Fig. 4. Normalized stress intensity factors for bimaterial system A at different normalized crack lengths (b/h_1) for Biot number ($Bi = \infty,\ 20$).

where γ_2 is the singularity at crack tip $b = h_1$ which can be obtained from Eq. (27), and $\sigma_{2yy}(x,0)$ is the stress in layer 2. Following Muskhelishvili (1953) and using Eqs. (20) and (25), the stress intensity factor at the crack tip can be evaluated from

$$K(b = h_1) = \frac{4\mu_2}{1+\kappa_2}\sqrt{2}\frac{d_{21} + d_{22}\gamma_2}{(h_1 - a)^{\gamma_1}\sin\pi\gamma_2}g(h_1), \tag{34}$$

where

$$d_{21} = \frac{m(\kappa_2+1)}{2(m+\kappa_1)} - \frac{3m(\kappa_2+1)}{2(m\kappa_2+1)},$$
$$d_{22} = \frac{m(\kappa_2+1)}{(m\kappa_2+1)} - \frac{m(\kappa_2+1)}{(m+\kappa_1)}, \quad m = \frac{\mu_1}{\mu_2}, \tag{35}$$

and if $a > 0 (b = h_1)$, the stress intensity factor at the crack tip a will be given by

$$K(a) = \frac{4\mu_1}{\kappa_1+1}\sqrt{2}\left(\frac{1}{h_1 - a}\right)^{\gamma_2} g(a). \tag{36}$$

In the formulation of the crack contact problem, we should include the crack contact length ε in the compressive zone as an additional unknown variable. The contact length would be calculated by using the smooth closure condition of the crack surface at $x = a$, which is assured by the condition $K(a) = 0$ (Bakioglu et al., 1976). So, the edge crack problem under thermal heating is solved as an embedded crack by fixing the crack length at $x = b$ and then determining by iteration the location of the crack tip $x = a$ at each time step such that the condition $K(a) = 0$ is satisfied. The numerical solution of the singular integral equation (20) is achieved by the expansion method developed in Kaya and Erdogan (1987a,b) and all the integrations appearing in the formulation are carried out numerically using the Jacobi–Gauss Quadrature formula and the Laguerre–Gauss Quadrature formula given in Stroud and Secrest (1966).

3. Results and discussion

In this study, the typical results for the layered medium are carried out for two different bimaterial systems, namely A and B. Table 1 gives the ratio of the thermoelastic properties of the two material pairs for each bimaterial system since the problem is formulated in terms of normalized quantities. The system A is made of a stainless steel (layer 1) welded onto a ferritic steel (layer 2) while system B is fabricated from a ceramic (layer 1) bonded to a ferritic steel (layer 2).

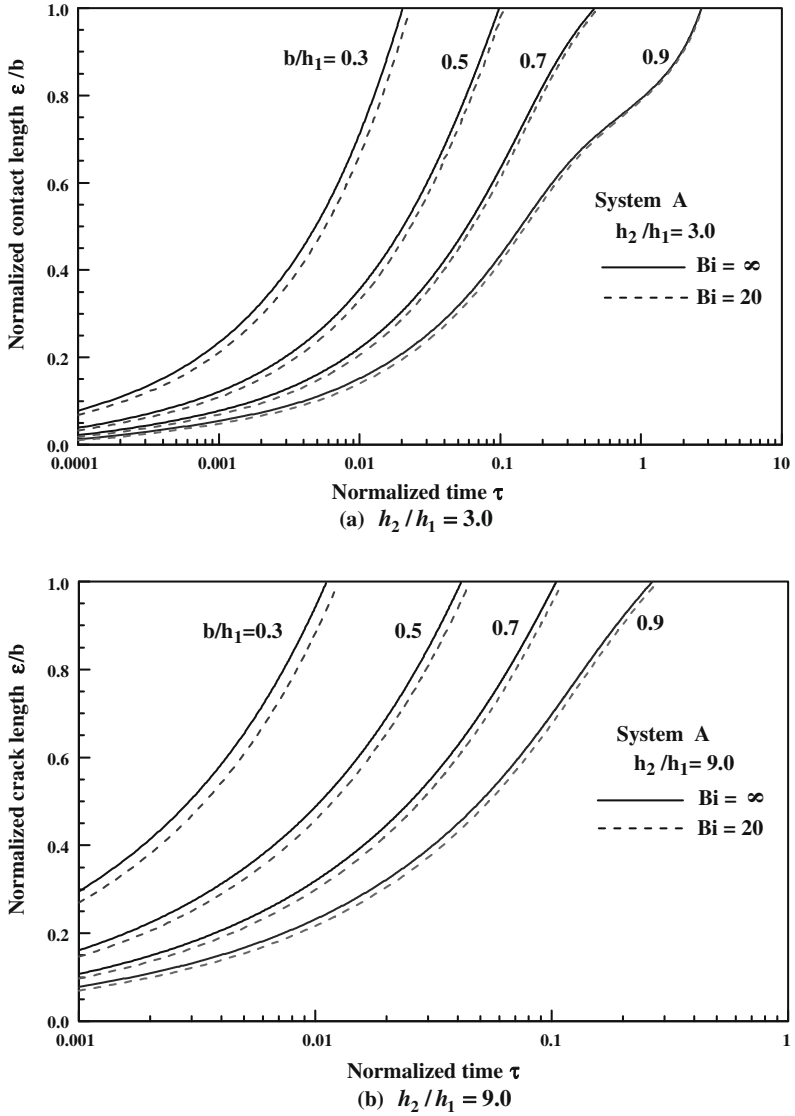

Fig. 5. Normalized crack contact length for bimaterial system A, at different normalized crack lengths (b/h_1), for Biot number ($Bi = \infty,\ 20$).

Figs. 2 and 3 demonstrate sample results for the normalized transient thermal stresses calculated from Eq. (4) and defined by $(\sigma^T_{yy}(x^*,\tau)/\sigma^T_o)$, where $\sigma^T_o = E_1\alpha'_1\theta_o/(1-\upsilon_1)$. These are displayed versus the normalized coordinate distance $x^* = x/h_1$ for both bimaterial systems A and B, some values of Fourier number, and two values of thickness ratio $h_2/h_1 = 3.0,\ 9.0$. The results are presented only for the unit step function temperature change at the boundary $x = 0$ and the values of Biot number ($Bi = \infty, Bi = hh_1/k'_1$), since it is the most severe case. For small values of Fourier number τ, the normalized thermal stresses, for both bimaterial systems A and B, start to be negative (compressive stresses) near the heating surface (layer 1) and near the insulated surface (layer 2), while the stresses are positive (tensile stresses) within layer 1 and layer 2. As the Fourier number τ grows, the behavior of the normalized thermal stresses for system A would be different than for system B. Indeed, for system A, as the time increases, the compressive zone will be increasing in layer 1 to be totally under compressive stresses as $\tau \to \infty$ (steady state) whereas layer 2 would be maintained under tensile stresses in the interior ($h_1 \leqslant x < h_1 + h_2$) and compressive stresses near the insulated surface ($h_1 < x \leqslant h_1 + h_2$). However, for system B, the compressive zone in layer 1 starts to increase as the time increases and then decreases to be totally under tensile stresses as $\tau \to \infty$ (steady state) while layer 2 would be under thermal stresses opposite to the initial behavior, i.e. compressive stresses in the interior ($h_1 \leqslant x < h_1 + h_2$) and tensile stresses near the insulated surface ($h_1 < x \leqslant h_1 + h_2$). Note that, for the steady state case ($\tau \to \infty$), the normalized thermal stress distribution becomes a linear function of x which can be shown from Eq. (4) with discontinuity at the interface due to the dissimilarity of the thermoelastic properties of the bimaterial systems. Also one can observe that, at any instant of time, the conditions of the zero resultant force and resultant moment at any cross-section are satisfied. During the initial very small time increments, the gradient of the normalized transient thermal stresses is very high and becomes lower as the time increases. The influence of the thickness ratio h_2/h_1 on the normalized thermal stresses is also shown in the same figures.

The variation of the normalized stress intensity factors for an edge crack problem ($b/h_1 < 1$) defined by $K(b)/\sigma^T_o\sqrt{b}$ and the variation of the normalized crack contact length ε/b versus Fourier number $\tau = tD_1/h_1^2$ are presented in Figs. 4–7. The numerical results are presented for the two bimaterial systems A and B, two values of thickness ratio $h_2/h_1 = 3.0,\ 9.0$, two values of Biot number $Bi = \infty,\ 20$ and some values of normalized crack length ($b/h_1 = 0.3,\ 0.5,\ 0.7,\ 0.9$). Figs. 4 and 5 correspond to system A while Figs. 6 and 7 stand for system B. For system A, the normalized stress intensity factors are shown in Fig. 4a, b and the corre-

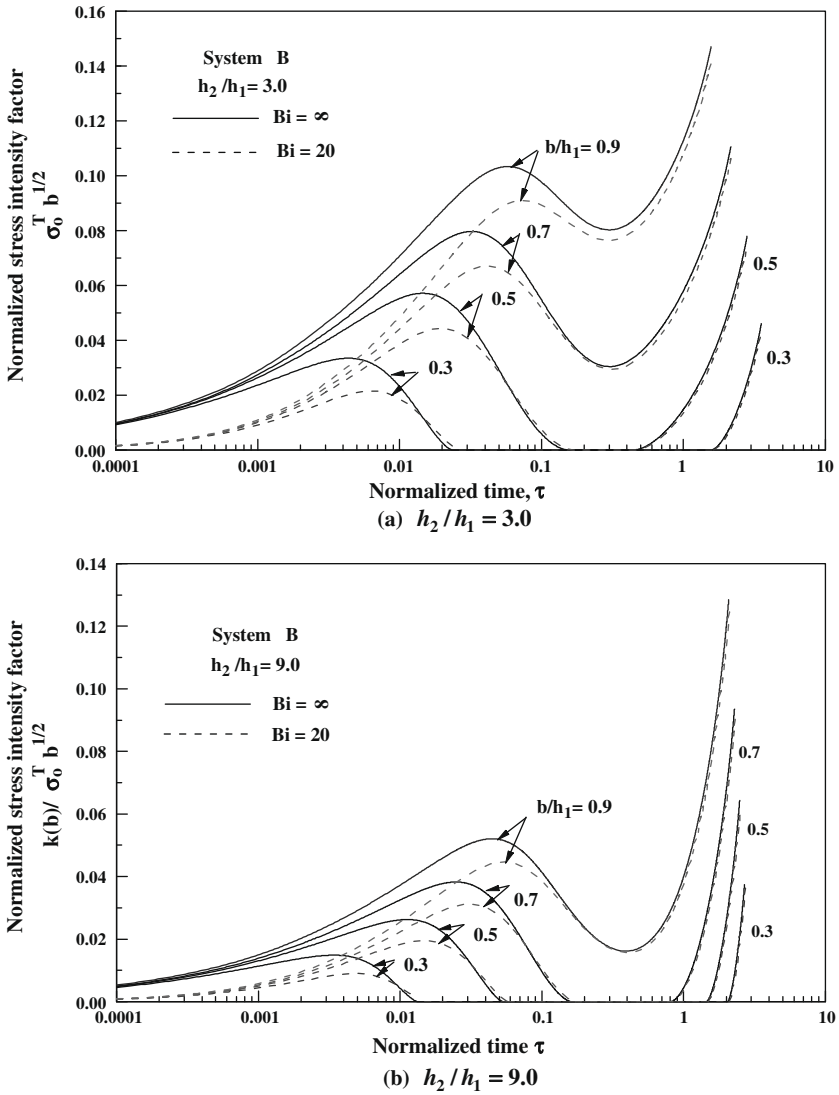

Fig. 6. Normalized stress intensity factors for bimaterial system B, at different normalized crack lengths (b/h_1), for Biot number ($Bi = \infty,\ 20$).

sponding normalized crack contact lengths are depicted in Fig. 5a, b. It is clear that the normalized stress intensity factor increases to a maximum value as τ increases and then it decreases to zero as the medium reaches a steady state condition ($\tau \to \infty$) for all normalized crack lengths and Biot numbers. By examining Fig. 5a, b we can observe that, for all crack lengths, a complete crack closure over the entire length of the crack ($\varepsilon = b$) will mainly occur due to the thermal stress distribution in layer 1, as shown in Fig. 2a, b. As the normalized crack length increases, the normalized stress intensity factor increases as well and delays the time in which the maximum value is reached. The opposite occurs when the plate surface is cooled (Rizk, 2008). So, the thermal fracture with surface heating, especially for a long crack, is more significant than for the cooled surface. The influence of the Biot number ($Bi = hh_1/k_1'$) and the thickness ratio (h_2/h_1) is also shown in the same figures by reducing the normalized stress intensity factors as the Biot number decreases and the thickness ratio increases. Note that the Fourier number needed to reach a full crack contact length also increases as the Biot number decreases.

For system B, Fig. 6a, b represent the variation of the normalized stress intensity factors while Fig. 7a, b stand for the associated normalized crack contact length. It is apparent that the variation of the normalized stress intensity factor, as well as the normalized crack contact length for system B, is completely different than for system A. Note that, the results in these figures are shown only for the cases where the crack contact length exist ($\varepsilon > 0$). It can be seen that the normalized stress intensity factor starts to increase to a maximum value as τ increases, then decreases, and finally increases again as normalized time τ increases. This performance is mainly a result of the thermal stress distribution in layer 1, as

Table 2
Normalized stress intensity factors $K(b)/\sigma_o^T\sqrt{b}$ for an edge crack ($b/h_1 < 1$) and $K(b)/\sigma_o^T b^{\gamma_2}$ for the crack terminating at the interface ($b/h_1 = 1$) for bimaterial system B at steady state condition ($\tau \to \infty$); $h_2/h_1 = 3.0,\ 9.0$.

b/h_1	$h_2/h_1 = 3.0$	$h_2/h_1 = 9.0$
$K(b)/\sigma_o^T\sqrt{b}$ $(\tau \to \infty)$		
0.3	0.2022	0.7740
0.5	0.2821	0.8193
0.7	0.3776	0.8793
0.9	0.5134	0.9772
$K(b)/\sigma_o^T b^{\gamma_2}$ $(\tau \to \infty)$		
1.0	0.3724	0.6355

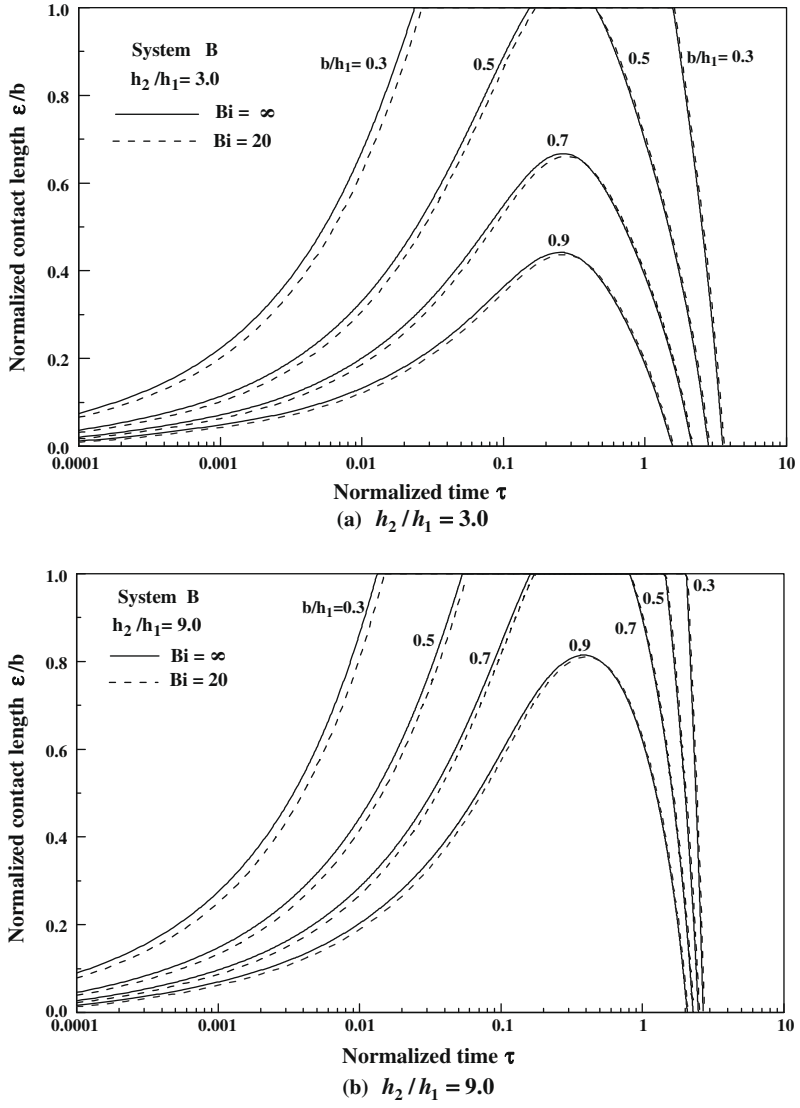

Fig. 7. Normalized crack contact length for bimaterial system B, at different normalized crack lengths (b/h_1), for Biot number ($Bi = \infty,\ 20$).

shown in Fig. 3a, b. It can be seen in Fig. 7a that, for $h_2/h_1 = 3.0$ and for $b/h_1 = 0.3,\ 0.5$, a complete crack closing over the entire length of the crack ($\varepsilon = b$) occurred for a period of time, after which it started to open again until it reached a fully edge crack case ($\varepsilon = 0,\ a = 0$) while for larger cracks ($b/h_1 = 0.7,\ 0.9$), a partial crack contact length over the whole crack length ($\varepsilon < b$) will take place at which the normalized stress intensity factor has a minimum value. In case of $h_2/h_1 = 9.0$, a complete crack closure ($\varepsilon = b$) is occurred for $b/h_1 = 0.3,\ 0.5,\ 0.7$ and partial crack contact length ($\varepsilon < b$) will be happening for $b/h_1 = 0.9$. It appeared in these figures that the stress intensity factor for $h_2/h_1 = 3.0$ is greater than for $h_2/h_1 = 9.0$. Also, as the normalized crack length b/h_1 increases, the values of the normalized stress intensity factor increases and is delayed. The effect of the Biot number is also shown in the figures by reducing the normalized stress intensity factors as the Biot number decreases. When the problem reaches the edge crack case ($\varepsilon = 0,\ a = 0$), and by observing the thermal stresses shown in Fig. 3, the normalized stress intensity factor calculated from Eq. (32) would increase as the normalized time (τ) increases until it reaches the steady state case ($\tau \to \infty$). The results for the normalized stress intensity factor at the steady state case ($\tau \to \infty$) are presented in Table 2. We can see from Table 2 that the normalized stress intensity factor increases as the normalized crack length increases and the results obtained for $h_2/h_1 = 9.0$ are higher than the results obtained for $h_2/h_1 = 3.0$. This is because the steady state thermal stress distribution in layer 1 for $h_2/h_1 = 9.0$ is greater than for $h_2/h_1 = 3.0$ as shown in Fig. 3.

The normalized stress intensity factors and the normalized crack contact length for the crack terminating at the interface ($b/h_1 = 1.0$) defined by Eq. (34) are depicted in Figs. 8,9 for the two bimaterial systems A and B, some values of Biot number ($Bi = \infty,\ 20,\ 10,\ 5$) and two values of thickness ratio $h_2/h_1 = 3.0,\ 9.0$. Observe that the results depicted in Figs. 8 and 9 are only for the edge-crack contact lengths ($\varepsilon > 0$). Since the adjacent materials for system A have the same mechanical properties ($E_1 = E_2,\ \upsilon_1 = \upsilon_2$), then the singularity at the crack tip ($b = h_1$) would be $\gamma_2 = 1/2$ while for system B the mechanical properties are different and the singularity at the crack tip would be $\gamma_2 = 0.552538$ which can be calculated from Eq. (27). The influence of the Biot number on the normalized stress intensity factors is made obvious since the stress intensity factors are reduced as the Biot number decreases. The results for system A are depicted in Fig. 8a, b which show a complete crack closure over the entire crack length ($\varepsilon = b$). The influence of the thickness ratio on the normalized stress intensity factors is also shown in the figures. For system B, Fig. 9a demonstrates the variation of the normalized stress intensity factors and Fig. 9b illustrates the corresponding normalized crack contact length. A partial crack contact length over the whole crack length ($\varepsilon < b$) will occur and then it starts to open again until it reaches the fully edge crack case

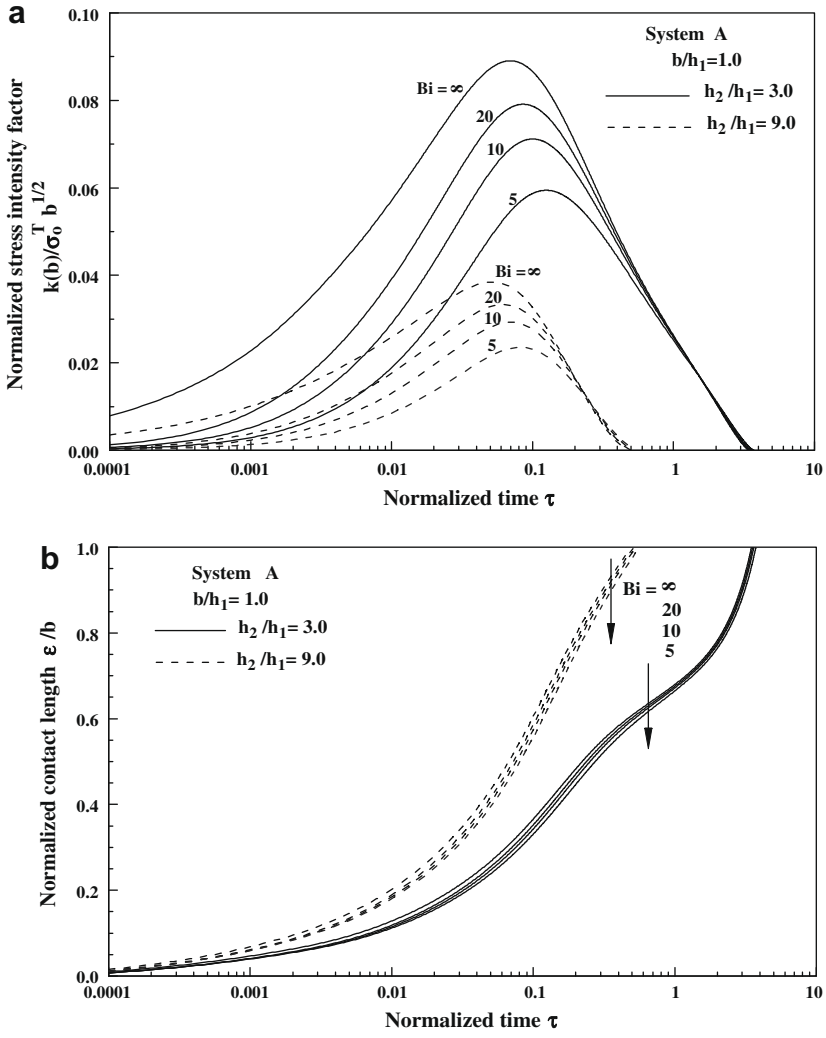

Fig. 8. (a) Normalized stress intensity factors (b) normalized crack contact length; for bimaterial system A at different Biot number, for crack terminating at the interface ($b/h_1 = 1$).

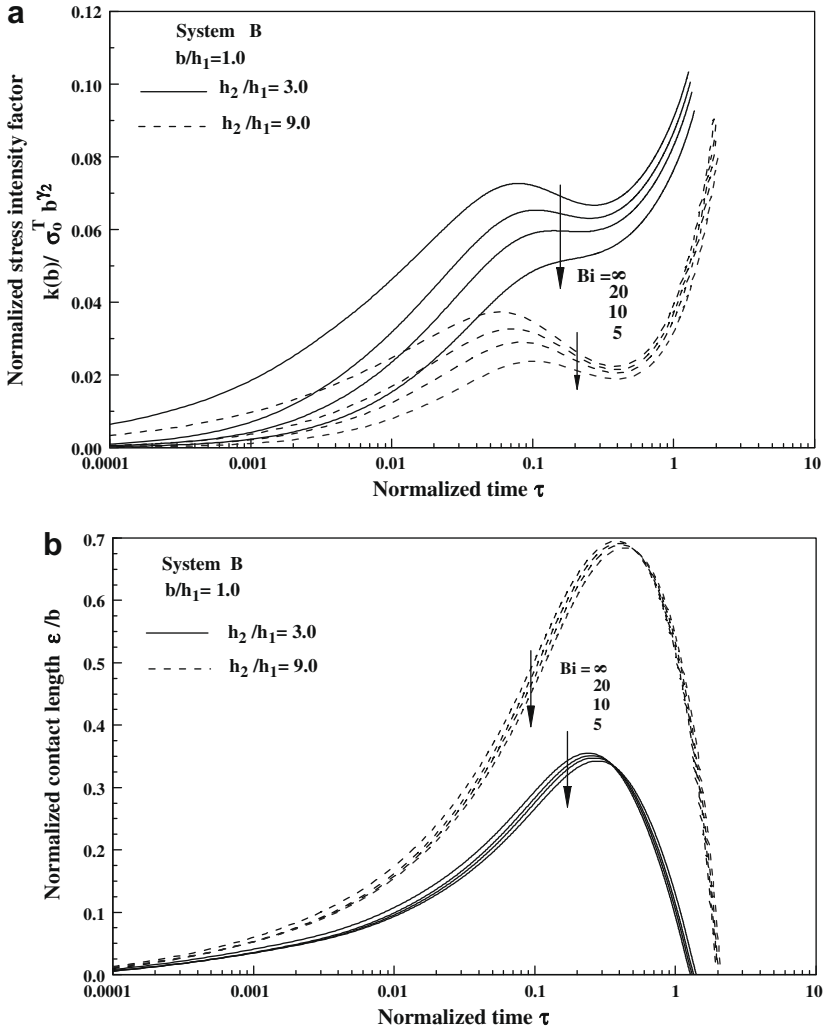

Fig. 9. (a) Normalized stress intensity factors (b) normalized crack contact length; for bimaterial system B at different Biot number, for crack terminating at the interface ($b/h_1 = 1$).

($\varepsilon = 0,\ a = 0$). The results of normalized stress intensity factors for the steady state fully edge crack problem ($\tau \to \infty$) are presented in Table 2. It seems that, the normalized stress intensity factor obtained for the thickness ratio $h_2/h_1 = 9.0$ is greater than for $h_2/h_1 = 3.0$ which mainly as a result of the steady state thermal stress distribution in layer 1 shown in Fig. 3.

Our purpose in solving this problem is to enable the prediction of failure for bonded dissimilar materials by providing the solution needed for assessing the crack propagation and arrest process in a coated medium containing a certain initial flaw and subjected to thermal loading. This requires the determination of the stress intensity factors as functions of time and dimensions concerning the size of the crack.

For system B, the results displayed in Fig. 6 show that the normalized stress intensity factor started to increase with time followed by a sharp decrease and finally an increase again to reach a maximum value at the steady state condition ($\tau \to \infty$). The results of these maximum normalized stress intensity factors are presented in Table 2. Usually, an important mode of mechanical failure in such materials is the subcritical crack growth. The cracks generally start from microflaws near or at the interface, or at the surface and grow perpendicularly to the nominal interface. Whether further fracture propagation would be the cleavage of the adjacent medium (steel), debonding along the interface, or reflection back into the first medium (ceramic) may depend on the relative strength to load factor ratios for various possible fracture modes. A fracture criterion based on the maximum stress concept has been proposed in Cook and Erdogan (1972) and can very well be applied here to determine if failure at the interface is imminent and if so what possible mode of crack propagation will take place. Validity of this criterion would have to be established by experimental studies.

4. Conclusion

The thermoelastic properties of the bimaterial systems have a great influence on the transient thermal stresses and consequently on the resulting stress intensity factors. For system A, a crack contact length increases as the normalized time increases and a complete crack closure occurred as $\tau \to \infty$ (steady state). The corresponding stress intensity factor increases to a maximum value after short time and then decreases to zero. For system B, the situation is different, in which a fully edge crack contact length occurs for a short crack while a partial crack contact length occurs for deep cracks and as τ increases it is opened once again to become fully edge crack case. The normalized stress intensity factor started to increase with time followed by a sharp decrease and finally an increase again to reach a maximum value at the steady state condition ($\tau \to \infty$). Also, the results of the normalized stress

intensity factor for surface heating are increasing as the normalized crack length increases, in contrast to those obtained for surface cooling. So, in the thermal cycling process, we should take into consideration the changes in the stress intensity factor for both cooling and heating, particularly for deep cracks. The effect of the Biot number is quite significant on the stress intensity factor by decreasing it as the Biot number decreases. Also, as the thickness ratio increases, the stress intensity factor decreases for both bimaterial systems as long as the crack contact length exists but, in case of a steady state condition, the stress intensity factor for system B becomes larger as the thickness ratio increases.

Acknowledgements

The authors gratefully acknowledge the financial support provided by the Ministry of Higher Education Malaysia (Grant No. FRGS 0207-62). In addition, thanks are due to Mrs. Lynn Mason for her help in editing this manuscript.

References

Bakioglu, M., Erdogan, F., Hesselman, D.P.H., 1976. Fracture mechanical analysis of self fatigue in surface compression strengthened glass plates. Journal of Material Science 11, 1826.

Burgreen, D., 1971. Elements of Thermal Stress Analysis. C.P. Press, Jamaica, New York.

Choi, H.J., 2003. Thermoelastic problem of steady state heat flow disturbed by a crack perpendicular to the graded interfacial zone in bonded materials. Journal of Thermal Stresses 26, 997–1030.

Choi, H.J., Jin, T.E., Lee, K.Y., 1995. Transient thermal stresses in a cladded semi-infinite medium containing an underclad crack. Journal of Thermal Stresses 18, 269–290.

Choi, H.J., Jin, T.E., Lee, K.Y., 1998. Collinear cracks in a layered half-plane with a graded nonhomogeneous interfacial zone-part II: Thermal shock response. International Journal of Fracture 94, 123–135.

Cook, H.C., Erdogan, F., 1972. Stresses in bonded materials with a crack perpendicular to the interface. International Journal of Engineering Science 10, 677–697.

Erdogan, F., Rizk, A.A., 1992. Fracture of coated plates and shells under thermal shock. International Journal of Fracture 53, 159–185.

Fan, X., Yu, S., 1992. Thermal shock in a surface-cracked plate. Engineering Fracture Mechanics 41, 223–228.

Ikeda, T., Sun, C.T., 2001. Stress intensity factor analysis for an interface crack between dissimilar isotropic materials under thermal stress. International Journal of Fracture 111, 229–249.

Itou, S., 2004. Thermal stresses around a crack in the nonhomogeneous interfacial layer between two dissimilar elastic half-planes. International Journal of Solids and Structures 41, 923–945.

Itou, S., Rengen, Q., 1993. Thermal stresses around two parallel cracks in two bonded dissimilar elastic half-planes. Archive of Applied Mechanics 63, 377–385.

Kaya, A.C., Erdogan, F., 1987a. On the solution of integral equations with strongly singular kernels. Quarterly of Applied Mathematics 45, 105–122.

Kaya, A.C., Erdogan, F., 1987b. On the solution of integral equations with generalized Cauchy kernels. Quarterly of Applied Mathematics 45, 455–469.

Lam, K.Y., Tay, T.E., Yuan, W.G., 1992. Stress intensity factors of cracks in finite plates subjected to thermal loading. Engineering Fracture Mechanics 43, 641–650.

Muskhelishvili, N.I., 1953. Singular Integral Equations. Noordhoff, Groningen, The Netherlands.

Nied, H.F., 1983. Thermal shock in an edge-cracked plate. Journal of Thermal stresses 1, 217–227.

Nied, H.F., 1987. Thermal shock in an edge-cracked plate subjected to surface heating. Engineering Fracture Mechanics 26, 239–246.

Pecht, M., 1991. Handbook of Electronic Package Design. CRC Press, New York.

Rizk, A.A., 1993. A cracked plate under transient thermal stresses due to surface heating. Engineering Fracture Mechanics 45, 687–696.

Rizk, A.A., 2004. Periodic array of cracks in strip subjected to surface heating. International Journal of Solids and Structures 41, 4685–4696.

Rizk, A.A., 2005. Convective thermal shock of infinite plate with periodic cracks. Journal of Thermal Stresses 28, 103–119.

Rizk, A.A., 2008. Stress intensity factor for an edge crack in two bonded dissimilar materials under convective cooling. Theoretical and Applied Fracture Mechanics 49, 251–267.

Rizk, A.A., Erdogan, F., 1989. Cracking of coated materials under transient thermal stresses. Journal of Thermal Stresses 12, 125–168.

Rizk, A.A., Radwan, S.F., 1993. Fracture of a plate under transient thermal stresses. Journal of Thermal Stresses 16, 79–102.

Stroud, A., Secrest, D., 1966. Gaussian Quadrature Formulas. Prentice-Hall, New York.

Zudin, Y.B., 2007. Theory of Periodic Conjugate Heat Transfer. Springer, Berlin.